ORGANOMETALLICS

Volume 6, Number 1, January 1987

Phenylation Reactions with Triosmium Carbyne and Carbene Cluster Complexes. The Crystal Structure of $Os_3(CO)_8(\mu_3,\eta^5\text{-}C(OMe)C(1,2\text{-}C_6H_4CPh))$, a Cluster Complex Containing an Osmacyclopentadiene System Linked to a Fischer-Type Carbene Ligand

Wen-Yann Yeh and John R. Shapley*

Department of Chemistry, University of Illinois, Urbana, Illinois 61801

Joseph W. Ziller and Melvyn Rowen Churchill*

Department of Chemistry, University at Buffalo, State University of New York, Buffalo, New York 14214

Received May 13, 1986

The dibenzylidyne complex $Os_3(CO)_9(\mu_3\text{-}CPh)_2$ (1) has been prepared by sequential treatment of $(\mu\text{-}H)Os_3(CO)_{10}(\mu_3\text{-}CPh)$ with PhLi and $MeOSO_2CF_3$. Similar Ph^-/Me^+ treatment of $(\mu\text{-}H)Os_3(CO)_9(\eta^1\text{-}C(OMe)_2)(\mu_3\text{-}CPh)$ leads to the related product $Os_3(CO)_8(\eta^1\text{-}C(OMe)_2)(\mu_3\text{-}CPh)_2$ (2) but also forms the products $Os_3(CO)_8(\mu_3,\eta^5\text{-}C(OMe)C(1,2\text{-}C_6H_4CPh))$ (3) and $Os_3(CO)_8(\mu_3,\eta^5\text{-}C(O)(OMe)C(1,2\text{-}C_6H_4CPh))$ (4). These compounds have been isolated as solids and have been characterized by IR, ^1H and ^{13}C NMR, and mass spectroscopies. The structure of 3 has been established by X-ray crystallography. $Os_3(CO)_8(\mu_3,\eta^5\text{-}C(OMe)C(1,2\text{-}C_6H_4CPh))$ crystallizes in the centrosymmetric monoclinic space group $P2_1/c$ with $a = 16.660$ (7) Å, $b = 10.439$ (4) Å, $c = 14.374$ (5) Å, $\beta = 98.94$ (3)°, $V = 2469.4$ (17) Å^3, and $Z = 4$. Diffraction data (Mo Kα, $2\theta = 4.0\text{–}45.0°$) were collected with a Syntex $P2_1$ automated four-circle diffractometer, and the structure was solved by a combination of direct methods (MULTAN) and difference-Fourier techniques. Refinement converged with $R_F = 5.4\%$ and $R_{wF} = 4.1\%$ for all 3245 unique data ($R_F = 3.5\%$ and $R_{wF} = 3.7\%$ for those 2491 data with $|F_o| > 6\sigma(|F_o|)$. The three osmium atoms define a triangular cluster in which Os(1)–Os(2) = 2.754 (1) Å, Os(1)–Os(3) = 2.903 (1) Å, and Os(2)–Os(3) = 2.720 (1) Å. Os(1) and Os(3) are each associated with three terminal carbonyl ligands, whereas Os(2) bears only two such ligands. The $\mu_3,\eta^5\text{-}(C(OMe)C(1,2\text{-}C_6H_4CPh))$ ligand is bound in a complex manner to the triosmium cluster. The initial carbon atom, C(1), is involved in an alkylidene linkage to Os(1) (Os(1)=C(1) = 2.065 (13) Å) and is linked to a methoxy group and to the second atom, C(3), with C(1)–C(3) = 1.449 (20) Å; C(3) bridges Os(2) and Os(3) (Os(2)–C(3) = 2.240 (12) Å and Os(3)–C(3) = 2.117 (13) Å) and is linked to a C_6H_4 fragment with C(3)–C(6A) = 1.399 (18) Å; the third carbon atom, C(4), bridges Os(2) and Os(3) (Os(2)–C(4) = 2.162 (14) Å and Os(3)–C(4) = 2.161 (14) Å), is linked to the C_6H_4 fragment with C(4)–C(6F) = 1.412 (20) Å, and is also bound to the phenyl group with C(4)–C(6G) = 1.532 (20) Å. In addition, C(6A) and C(6F) of the $1,2\text{-}C_6H_4$ ligand are bonded to Os(2) with Os(2)–C(6A) = 2.331 (12) Å, Os(2)–C(6F) = 2.326 (13) Å, and C(6A)–C(6F) = 1.444 (20) Å. The Os(3)–C(3)–C(6A)–C(6F)–C(4) system is planar and behaves as an osmacyclopentadiene ligand in its binding to Os(2).

Transition-metal alkylidene (carbene) and alkylidyne (carbyne) complexes in low oxidation states are sometimes closely interrelated, such that alkylidene groups can be converted into alkylidyne groups and vice versa.[1] Thus, a two-step H^-/H^+ procedure effects the alkylidyne transformation of $(\mu\text{-}H)Os_3(CO)_{10}(\mu\text{-}COMe)$ to $(\mu\text{-}H)Os_3(CO)_{10}(\mu_3\text{-}CH)$ via an alkylidene intermediate, $[(\mu\text{-}H)Os_3(CO)_{10}(\mu\text{-}CHOMe)^-]$.[2] In contrast, we found that an analogous Ph^-/Me^+ treatment of $(\mu\text{-}H)Os_3(CO)_{10}(\mu\text{-}COMe)$ is more complex, with the initial attack occurring at a carbonyl ligand, leading to a mixed alkylidene–alkylidyne complex, $(\mu\text{-}H)Os_3(CO)_9(\eta^1\text{-}C(OMe)_2)(\mu_3\text{-}CPh)$.[3] However, extended treatment of this intermediate with $MeOSO_2CF_3$

(1) Fischer, H.; Motsch, A.; Markl, R.; Ackemann, K. *Organometallics* **1985**, *4*, 726 and references therein.

(2) Shapley, J. R.; Cree-Uchiyama, M. E.; St. George, G. M.; Churchill, M. R.; Bueno, C. *J. Am. Chem. Soc.* **1983**, *105*, 140.

(3) Shapley, J. R.; Yeh, W.-Y.; Churchill, M. R.; Li, Y.-J. *Organometallics* **1985**, *4*, 1898.

0276-7333/87/2306-0001$01.50/0

Scheme I

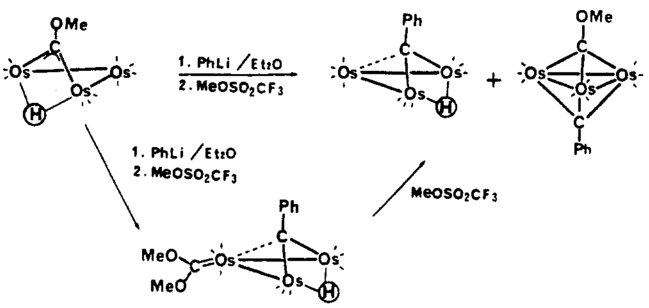

gives the initially expected complex, $(\mu\text{-H})Os_3(CO)_{10}(\mu_3\text{-CPh})$,[4] together with a coproduct, $Os_3(CO)_9(\mu_3\text{-CPh})(\mu_3\text{-COMe})$[5] (see Scheme I). In order to probe the generality of this sequential Ph^-/Me^+ treatment, we have investigated its effect on different triosmium alkylidyne and alkylidene systems. Presented in this paper are results concerning the reactions with $(\mu\text{-H})Os_3(CO)_{10}(\mu_3\text{-CPh})$[4] and $(\mu\text{-H})Os_3(CO)_9(\eta^1\text{-C(OMe)}_2)(\mu_3\text{-CPh})$[3] (see Scheme II).

Experimental Section

General Procedures. $(\mu\text{-H})Os_3(CO)_{10}(\mu_3\text{-CPh})$[4] and $(\mu\text{-H})Os_3(CO)_9(\eta^1\text{-C(OMe)}_2)(\mu_3\text{-CPh})$[3] were prepared by the methods described previously. Phenyllithium (Alfa, 1.8 M in ether–benzene) and methyl trifluoromethanesulfonate (Aldrich) were used directly as received. Diethyl ether was distilled from sodium benzophenone ketyl before use. Preparative thin-layer chromatographic (TLC) plates were prepared from Silica Gel GF (Type 60, E. Merck). Melting points were determined in sealed capillaries. ^1H NMR (360 MHz) spectra were obtained on a Nicolet NT-360 spectrometer. ^{13}C NMR (90.56 MHZ) spectra were also obtained on the Nicolet NT-360 spectrometer on samples resulting from ^{13}C-enriched triosmium cluster starting materials. IR spectra were taken on a Perkin-Elmer 281 B spectrometer and were calibrated with polystyrene film and cyclohexane (2138.5 cm^{-1}). Elemental analyses were performed by the Microanalytical Laboratory of the School of Chemical Sciences at the University of Illinois. Field desorption mass spectra were obtained by the staff of the Mass Spectroscopy Laboratory of the School of Chemical Sciences (Illinois) on a Varian-MAT 731 mass spectrometer.

Sequential Ph^-/Me^+ Treatment of $(\mu\text{-H})Os_3(CO)_{10}(\mu_3\text{-CPh})$. An oven-dried, 50-mL Schlenk flask was equipped with a magnetic stir bar and a rubber serum stopper. $(\mu\text{-H})Os_3(CO)_{10}(\mu_3\text{-CPh})$ (109 mg, 0.116 mmol) was added against a nitrogen flow. Freshly distilled diethyl ether (30 ml) was then introduced by cannula. After the mixture was cooled to 0 °C in an ice bath, phenyllithium (193 μL, 0.348 mmol) was added via a syringe over a period of 15 min, and the mixture was then stirred for 30 min. Methyl trifluoromethanesulfonate (98 μL, 0.87 mmol) was added to the resulting orange-yellow mixture via a syringe. The solution was concentrated slowly to ca. 5 mL under vacuum at 0 °C, placed under nitrogen, and stirred at 25 °C for 46 h. The mixture was subjected to TLC, eluting with *n*-pentane. Isolation of the material forming the first, orange-red band recovered $(\mu\text{-H})Os_3(CO)_{10}(\mu\text{.CPh})$ (35 mg, 32%). Crystallization of the material forming the second, orange-red, band from dichloromethane–methanol, produced air-stable, dark red crystals of $Os_3(CO)_9(\mu_3\text{-CPh})_2$ (1) (34 mg, 0.033 mmol, 29%). The five further bands were not identified.

Characterization of 1. Mp: 139–140 °C; mass spectrum: *m/z* 1006 (M^+, ^{192}Os). IR (C_6H_{12}): ν(CO) 2064 (vs), 2057 (vs), 2022 (s), 2002 (sh, br), 1992 (m, br) cm^{-1}. ^1H NMR (CD_3CN, 17 °C): δ 8.00 (d, 4 H, J = 7 Hz, C_6H_5 (ortho)), 7.40 (t, 4 H, J = 7 Hz, C_6H_5 (meta)), 7.32 (t, 2 H, J = 7 Hz, C_6H_5 (para)). ^{13}C NMR ($CDCl_3$, 17 °C): δ 275.7 (s, ≡*C*-Ph), 174.9 (s, *C*O). Anal. Calcd for $Os_3C_{23}H_{10}O_9$: C, 27.58; H, 1.00. Found: C, 27.26; H, 1.34.

Sequential Ph^-/Me^+ Treatment of $(\mu\text{-H})Os_3(CO)_9(\eta^1\text{-C(OMe)}_2)(\mu_3\text{-CPh})$. An oven-dried, 100-mL Schlenk flask was equipped with a magnetic stir bar and a rubber serum stopper under a nitrogen atmosphere. The stopper was briefly removed, and first $(\mu\text{-H})Os_3(CO)_9(\eta^1\text{-C(OMe)}_2)(\mu_3\text{-CPh})$ (75 mg, 0.076 mmol) and then diethyl ether (30 ml) were added against a nitrogen flow. After the solution was cooled to 0 °C in an ice bath, phenyllithium (105 μL, 0.19 mmol) was added via a syringe over a period of 30 min. Then methyl trifluoromethanesulfonate (100 μL, 0.88 mmol) was added to the orange-yellow mixture via a syringe. The mixture was slowly concentrated to ca. 5 mL under vacuum at 0 °C and then placed under nitrogen and stirred at room temperature for 40 h. The volatile materials were removed under vacuum, and the residue was subjected to TLC, eluting with *n*-pentane–dichloromethane (9:1, v/v). Isolation of the material forming the first, orange-yellow, band gave $Os_3(CO)_9(\mu_3\text{-CPh})_2$ (1) (5 mg, 0.005 mmol, 6%). Crystallization of the second, orange-red, band from acetonitrile afforded air-stable, dark red crystals of $Os_3(CO)_8(\mu_3,\eta^5\text{-C(OMe)C(1,2-}C_6H_4\text{CPh))}$ (3) (24 mg, 0.024 mmol, 31%). Crystallization of the third, orange, band from pentane produced air-stable, orange-red crystals characterized as $Os_3(CO)_8(\mu_3,\eta^5\text{-C(O)(OMe)C(1,2-}C_6H_4\text{CPh))}$ (4) (13 mg, 0.013 mmol, 16%). Isolation of the material forming the fourth, pink, band produced an orange-yellow solid identified as $Os_3(CO)_8(\eta^1\text{-C(OMe)}_2)(\mu_3\text{-CPh})_2$ (2) (11 mg, 0.01 mmol, 14%).

$Os_3(CO)_8(\eta^1\text{-C(OMe)}_2)(\mu_3\text{-CPh})_2$ (2). Mass spectrum: *m/z* 1052 (M^+, ^{192}Os). IR (C_6H_{12}): ν(CO) 2076 (m), 2055 (sh), 2048 (vs), 2024 (s), 2010 (vs), 1984 (m), 1969 (m), 1940 (w) cm^{-1}. ^1H NMR (CD_3CN, 17 °C): δ 7.86 (d, 4 H, J = 7 Hz, C_6H_5 (ortho)), 7.33 (t, 4 H, J = 7 Hz, C_6H_5 (meta)), 7.24 (t, 2 H, J = 7 Hz, C_6H_5 (para)), 3.76 (s, 6 H, 2 CH_3). ^{13}C NMR ($CDCl_3$, −55 °C): δ 268.4 (s, ≡*C*Ph), 220.4 (s, = *C*(OMe)$_2$), 180.8 (s, 2 *C*O), 178.0 (s, 6 *C*O).

$Os_3(CO)_8(\mu_3,\eta^5\text{-C(OMe)C(1,2-}C_6H_4\text{CPh))}$ (3). Mass spectrum: *m/z* 1020 (M^+, ^{192}Os). IR (C_6H_{12}): ν(CO) 2080 (s), 2051 (vs), 2009 (vs), 2003 (vs), 1988 (m), 1967 (w), 1946 (m) cm^{-1}. ^1H NMR ($(CD_3)_2CO$, 17 °C): δ 7.84-7.34 (m, 9 H), 4.25 (s, 3 H). ^{13}C NMR ($CDCl_3$, -55 °C): δ 242.5 (s + dd, ^1J(C-C) = 31 Hz, ^2J(C-C) = 30 Hz, *C*-OMe), 191.5 (s, *C*-Ph), 184.6 (s + d, ^2J(C-C) = 30 Hz, *C*O), 181.2 (s, *C*O), 179.1 (s, *C*O), 178.0 (s, *C*O), 176.8 (s + d, ^2J(C-C) = 20 Hz, *C*O), 176.2 (s, *C*O), 173.9 (s, *C*O), 172.1 (s, *C*O), 100.8 (s + dd, ^1J(C-C) = 31 Hz, ^2J(C-C) = 20 Hz, *C*(C_6H_4CPh)). Anal. Calcd for $Os_3C_{24}H_{12}O_9$: C, 28.40; H, 1.19. Found: C, 28.41; H, 1.24. The crystal of 3 found suitable for an X-ray study was grown from acetonitrile at room temperature.

$Os_3(CO)_8(\mu_3,\eta^5\text{-C(O)(OMe)C(1,2-}C_6H_4\text{CPh))}$ (4). Mass spectrum: *m/z* 1036 (M^+, ^{192}Os). IR (C_6H_{12}): ν(CO) 2080 (m), 2053 (vs), 2009 (s), 2001 (vs), 1997 (s), 1988 (w), 1971 (w), 1939 (m) cm^{-1}. ^1H NMR ($CDCl_3$, 20 °C): δ 7.56–7.03 (m, 9 H), 4.00 (s, 3 H). Anal. Calcd for $Os_3C_{24}H_{12}O_{10}$: C, 27.96; H, 1.17. Found: C, 27.82; H, 1.30.

Collection of X-ray Diffraction Data and Structure Solution for $Os_3(CO)_8(\mu_3,\eta^5\text{-C(OMe)C(1,2-}C_6H_4\text{CPh))}$ (3). A bright red crystal of approximate dimensions 0.1 × 0.2 × 0.3 mm was cleaved from a larger crystal and sealed into a glass capillary. All orientation and indexing operations as well as room temperature (21 °C) data collection were carried out on the Syntex $P2_1$ automated four-circle diffractometer at SUNY—Buffalo by using the standard techniques of that laboratory.[6] Final cell parameters are based on a least-squares analysis of 25 reflections in well-separated regions of reciprocal space, all having $22° < 2\theta < 30°$. Details are given in Table I.

A careful survey of the data set revealed the systematic extinctions *h0l* for $l = 2n + 1$ and *0k0* for $k = 2n + 1$. The space group is thus uniquely defined as $P2_1/c$ (C^5_{2h}; No. 14).[7]

All 3245 unique reflections were converted to unscaled $|F_o|$ values following correction for absorption and for Lorentz and polarization effects. A Wilson plot was used to place the data on an approximate absolute scale. Any reflection with I(net) < 0 was assigned the value $|F_o| = 0$.

All subsequent crystallographic calculations were performed by using our locally modified version of the Syntex XTL inter-

(4) Yeh, W.-Y.; Shapley, J. R.; Li, Y.-J.; Churchill, M. R. *Organometallics* **1985**, *4*, 767.
(5) Yeh, W.-Y.; Shapley, J. R.; Ziller, J. W.; Churchill, M. R. *Organometallics* **1986**, *5*, 1757.
(6) Churchill, M. R.; Lashewycz, R. A.; Rotella, F. J. *Inorg. Chem.* **1977**, *16*, 265.
(7) *International Tables for X-Ray Crystallography*; Kynoch: Birmingham, England, 1965; Vol. 1, p 99.

Scheme II

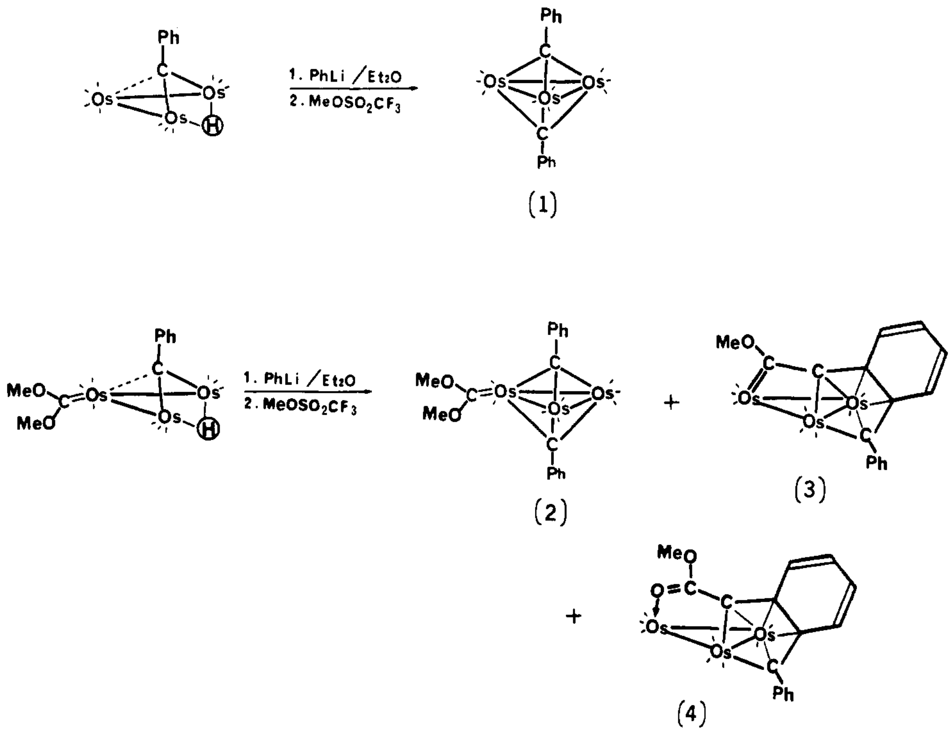

Table I. Experimental Data for the X-ray Diffraction Study of $Os_3(CO)_8(\mu_3\text{-}\eta^5\text{-}C(OMe)C(1,2\text{-}C_6H_4CPh))$

(A) Unit Cell Data at 21° (294 K)	
crystal system: monoclinic	space group: $P2_1/c$
a = 16.660 (7) Å	Z = 4
b = 10.439 (4) Å	formula = $C_{24}H_{12}O_9Os_3$
c = 14.374 (5) Å	
β = 98.937(33)°	D(calcd) = 2.73 cm^{-3}
V = 2469.4 (17) Å^3	
(B) Collection of X-ray Diffraction Data	
diffractometer	Syntex $P2_1$
radiation	Mo Kα ($\bar{\lambda}$ = 0.710 730 Å)
monochromator	highly oriented (pyrolytic) graphite; equatorial mode with 2θ(m) = 12.160°; assumed to be 50% perfect/50% ideally mosaic for polarization correction
reflections measured	$+h,+k,\pm l$ for 2θ = 4.0–45.0°; 3376 total, merged to 3245 unique data (filename OSOM-204)
scan type	coupled θ(crystal) – 2θ(counter)
scan width	$[2\theta(K\alpha_1) - 0.9]° \rightarrow [2\theta(K\alpha_2) + 0.9]°$
scan speed	4.0 deg min^{-1} (in 2θ)
standard reflections	three measured after each batch of 97 reflections; no significant fluctuations detected
absorption correction	μ(Mo Kα) = 163.7 cm^{-1}; corrected empirically by interpolation (in 2θ and ϕ) between ψ-scans of close-to-axial reflections

active program package[8] at SUNY—Buffalo. The structure was solved by direct methods using the program MULTAN;[9] the positions of the three osmium atoms were obtained from an "E-map". All other non-hydrogen atoms were located by using difference-Fourier syntheses and refined by full-matrix least-squares techniques. The function $\Sigma w(|F_o| - |F_c|)^2$ was minimized, where $1/w = \{\sigma(|F_o|)\}^2 + \{0.015|F_o|\}^2$. All hydrogen atoms were included in fixed (but constantly updated) calculated positions assuming d(C–H) = 0.95 Å.[10] Using anisotropic thermal parameters for all non-hydrogen atoms (325 parameters, data-to-parameter ratio = 10.0:1) the model converged[11] with R_f = 5.4%, R_{wF} = 4.1%, and GOF = 1.42 for all 3245 data (nonrejected). The residuals using only those 2772 data with $|F_o| > 3\sigma(|F_o|)$ were R_F = 4.1% and R_{wF} = 4.0% (R_F = 3.5%, R_{wF} = 3.7% for those 2491 data with $|F_o| > 6\sigma(|F_o|)$).

An analysis of the function $\Sigma w(|F_o| - |F_c|)^2$ showed no unusual trends as a function of Miller indices, $|F_o|$, $(\sin\theta)/\lambda$, or sequence number. A final difference-Fourier synthesis was featureless.

The analytical scattering factors of Cromer and Waber[12a] for neutral atoms were used throughout the analysis; both the real ($\Delta f'$) and imaginary ($i\Delta f''$) components of anomalous dispersion[12b] were specifically included for all non-hydrogen atoms.

Final positional parameters are collected in Table II. Anisotropic thermal parameters and a table of observed and calculated structure factor amplitudes appear as supplementary material.

Results and Discussion

Sequential Ph^-/Me^+ Treatment of $(\mu\text{-}H)Os_3(CO)_{10}(\mu_3\text{-}CPh)$. This two-step procedure effects a CO → CPh transformation (with deprotonation), leading to the dibenzylidyne complex $Os_3(CO)_9(\mu_3\text{-}CPh)_2$ (1) in 29% yield (see Scheme II). The starting material is recovered in 32% yield together with five uncharacterized coproducts. It is probable that initial Ph^- attack occurs at a carbonyl ligand and that Me^+ addition gives the intermediate species $HOs_3(CO)_9(\eta^1\text{-}C(OMe)Ph)(\mu_3\text{-}CPh)$. Prolonged exposure to Me^+ could then give both $(\mu\text{-}H)Os_3(CO)_{10}(\mu_3\text{-}CPh)$ and $Os_3(CO)_9(\mu_3\text{-}CPh)_2$ (1) via processes analogous to those involved in the transformation of $(\mu\text{-}H)Os_3(CO)_9(\eta^1\text{-}C(OMe)_2)(\mu_3\text{-}CPh)$ to $(\mu\text{-}H)Os_3(CO)_{10}(\mu_3\text{-}CPh)$ and $Os_3(CO)_9(\mu_3\text{-}CPh)(\mu_3\text{-}COMe)$ (see Scheme I).

Characterization of $Os_3(CO)_9(\mu_3\text{-}CPh)_2$ (1). Compound 1 is a red, crystalline solid. The simple IR ab-

(8) *Syntex XTL Operations Manual*, Syntex Analytical Instruments, 2nd ed., Cupertino, CA, 1976.

(9) (a) Germain, G.; Woolfson, M. M. *Acta Crystallogr. Sect. B* **1968**, *B24*, 91. (b) Germain, G.; Main, P.; Woolfson, M. M. *Acta Crystallogr. Sect. A* **1971**, *A27*, 368.

(10) Churchill, M. R. *Inorg. Chem.* **1973**, *12*, 1213.

(11) Discrepancy indices are defined as follows: R_F (%) = $100\sum||F_o| - |F_c||/\sum|F_o|$; R_{wF} (%) = $100[\sum w(|F_o| - |F_c|)^2/\sum w[F_o]^2]^{1/2}$; GOF = $[\sum w(|F_o| - |F_c|)^2/(NO - NV)]^{1/2}$, where NO = number of observations and NV = number of variables.

(12) *International Tables for X-Ray Crystallography*; Kynoch: Birmingham, England, 1974; Vol. 4: (a) pp 99–101; (b) pp 149–150.

Table II. Final Atomic Coordinates (with Esd's) for $Os_3(CO)_8(\mu_3,\eta^5$-C(OMe)C(1,2-C_6H_4CPh))

atom	*x*	*y*	*z*	*B*, Å^2
OS(1)	0.36830 (3)	0.30351 (6)	0.05527 (4)	
OS(2)	0.21164 (3)	0.39605 (5)	0.02437 (4)	
OS(3)	0.31606 (3)	0.51698 (5)	0.16061 (4)	
O(1)	0.28272 (58)	0.12391 (88)	0.18716 (72)	
O(11)	0.42163 (79)	0.4796 (15)	−0.09502 (95)	
O(12)	0.3438 (11)	0.0780 (14)	−0.0765 (11)	
O(13)	0.53737 (71)	0.2233 (13)	0.1463 (10)	
O(21)	0.12171 (93)	0.1850 (13)	−0.09526 (88)	
O(22)	0.21735 (67)	0.5305 (11)	−0.16028 (73)	
O(31)	0.47685 (66)	0.4279 (13)	0.28004 (84)	
O(32)	0.27858 (68)	0.6758 (12)	0.32726 (84)	
O(33)	0.39400 (81)	0.7326 (13)	0.05977 (95)	
C(1)	0.30010 (77)	0.2340 (15)	0.15253 (87)	
C(2)	0.3250 (10)	0.0082 (15)	0.1627 (13)	
C(3)	0.25340 (80)	0.3436 (12)	0.17527 (87)	
C(4)	0.18970 (82)	0.5586 (14)	0.11021 (94)	
C(6A)	0.16867 (73)	0.3474 (13)	0.16709 (80)	
C(6B)	0.11452 (83)	0.2422 (14)	0.1815 (10)	
C(6C)	0.03302 (95)	0.2588 (16)	0.1668 (11)	
C(6D)	−0.00071 (83)	0.3808 (16)	0.1384 (11)	
C(6E)	0.04593 (88)	0.4796 (14)	0.1192 (10)	
C(6F)	0.13309 (78)	0.4684 (14)	0.13402 (83)	
C(6G)	0.16213 (78)	0.6961 (13)	0.0854 (10)	
C(6H)	0.17925 (80)	0.7584 (14)	0.0056 (10)	
C(6I)	0.14956 (89)	0.8800 (13)	−0.0136 (11)	
C(6J)	0.1041 (10)	0.9420 (14)	0.0461 (13)	
C(6K)	0.08812 (90)	0.8794 (16)	0.1252 (11)	
C(6L)	0.11706 (86)	0.7558 (14)	0.1439 (10)	
C(11)	0.40137 (92)	0.4125 (20)	−0.0410 (13)	
C(12)	0.3565 (11)	0.1635 (19)	−0.0253 (13)	
C(13)	0.4733 (11)	0.2567 (16)	0.1094 (12)	
C(21)	0.1527 (10)	0.2647 (16)	−0.0496 (11)	
C(22)	0.21383 (83)	0.4771 (13)	−0.0899 (11)	
C(31)	0.4185 (10)	0.4597 (16)	0.2273 (11)	
C(32)	0.29365 (77)	0.6166 (15)	0.2666 (11)	
C(33)	0.36581 (94)	0.6552 (16)	0.0989 (11)	
H(6B)	0.1374	0.1591	0.2018	7.0
H(6C)	−0.0018	0.1875	0.1750	7.0
H(6D)	−0.0586	0.3936	0.1325	7.0
H(6E)	0.0203	0.5600	0.0957	7.0
H(6H)	0.2120	0.7166	−0.0356	7.0
H(6I)	0.1604	0.9236	−0.0708	7.0
H(6J)	0.0835	1.0282	0.0325	7.0
H(6K)	0.0567	0.9223	0.1683	7.0
H(6L)	0.1045	0.7106	0.1993	7.0
H(2A)	0.3068	−0.0655	0.1927	7.0
H(2B)	0.3827	0.0161	0.1824	7.0
H(2C)	0.3157	−0.0056	0.0961	7.0

sorption pattern in the carbonyl region for 1 reflects the symmetry of the expected structure in which the two benzylidyne ligands bridge the opposite triangular faces of the $Os_3(CO)_9$ moiety.[5]

The ^{1}H NMR spectrum of 1 is shown in Figure 1. On the basis of the ^{1}H–^{1}H couplings, the 4 H doublet at δ 8.00, the 4 H triplet at δ 7.40, and the 2 H triplet at δ 7.32 are assigned to the ortho, meta, and para protons, respectively, of the two equivalent groups. This pattern for the phenyl group, in which the ortho protons are shifted significantly downfield, has been previously noted for $(\mu$-H$)_3Os_3(CO)_9(\mu_3$-CPh),[4] $Os_3(CO)_9(\mu_3$-CPh$)(\mu_3$-COMe),[5] and $Cp_3M_3(\mu_3$-CPh$)_2$ (M = Co,[13] Rh,[14,15] Ir[15]).

The ^{13}C NMR spectrum of 1 at 17 °C shows the carbonyl carbons as a singlet at δ 174.9, which remains sharp to low temperature. This is presumably due to facile 3-fold ro-

(13) Fritch, J. R.; Vollhardt, K.P.C. *Angew. Chem., Int. Ed. Engl.* **1980**, *19*, 559.
(14) (a) Gardner, S. A.; Andrews, P. S.; Rausch, M. D. *Inorg. Chem.* **1973**, *12*, 2396. (b) Todd, L. J.; Wilkinson, J. R.; Rausch, M. D.; Gardner, S. A.; Dickson, R. S. *J. Organomet. Chem.* **1975**, *101*, 133.
(15) Clauss, A. D.; Shapley, J. R.; Wilker, C. N.; Hoffman, R. *Organometallics* **1984**, *3*, 619.

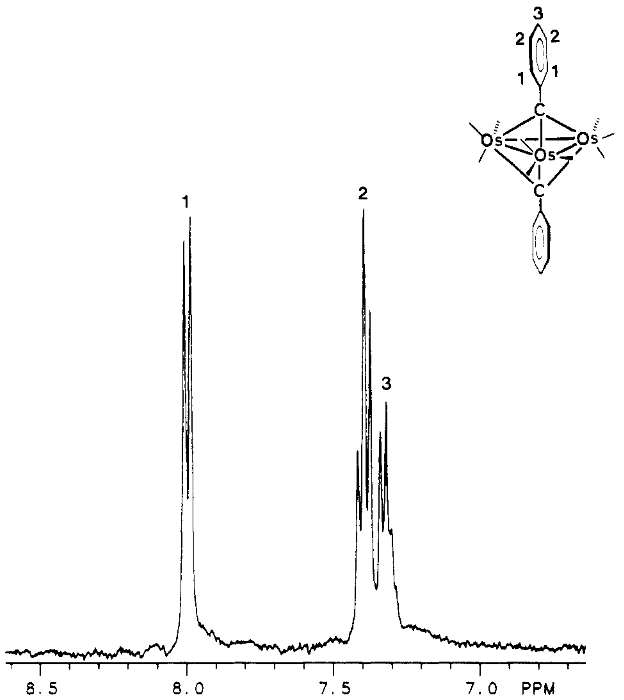

Figure 1. 360 MHz ^{1}H NMR spectrum of $Os_3(CO)_9(\mu_3$-CPh$)_2$ in CD_3CN at 17 °C.

tation in each $Os(CO)_3$ unit; similar behavior for the carbonyls is observed for $Os_3(CO)_9(\mu_3$-CPh$)(\mu_3$-COMe).[5] The benzylidyne carbon signal for 1 is at δ 275.5 and does not show temperature dependence. In contrast, the benzylidyne carbon resonance for $Os_3(CO)_9(\mu_3$-CPh$)(\mu_3$-COMe) is significantly upfield (δ 234.6), and the shift is quite temperature dependent.[5] However, the benzylidyne carbon resonances for these two compounds fall well within the range observed for two other triosmium benzylidyne complexes, namely, $(\mu$-H$)_3Os_3(CO)_9(\mu_3$-CPh) (δ 153.7)[4] and $(\mu$-H$)Os_3(CO)_{10}(\mu_3$-CPh) (δ 314.2).[4] The latter complex adopts a semi-triply-bridging configuration. Thus, the benzylidyne carbon chemical shift is quite sensitive to both its own binding mode and to its coligands on the triosmium framework.

Sequential Ph$^-$/Me$^+$ Treatment of $(\mu$-H$)Os_3(CO)_9(\eta^1$-C(OMe)$_2)(\mu_3$-CPh). This treatment leads to three major products, $Os_3(CO)_8(\eta^1$-C(OMe)$_2)(\mu_3$-CPh$)_2$ (2) (14%), $Os_3(CO)_8(\mu_3,\eta^5$-C(OMe)C(1,2-C_6H_4CPh)) (3) (31%), and $Os_3(CO)_8(\mu_3,\eta^5$-C(O)(OMe)C(1,2-C_6H_4CPh)) (4) (16%) (see Scheme II). Again, initial Ph$^-$ attack probably occurs at a carbonyl ligand, and Me$^+$ addition may generate a mixed dialkylidene–alkylidyne species, $(\mu$-H$)Os_3(CO)_8(\eta^1$-C(OMe)$_2)(\eta^1$-C(OMe)Ph$)(\mu_3$-CPh). However, the subsequent transformations to the final products must involve a complicated sequence of rearrangements which are generally unclear at present.

Characterization of Compound 2. On the basis of IR, ^{1}H, and ^{13}C NMR data, 2 appears to have a similar structure with the compound $Os_3(CO)_8(PPh_3)(\mu_3$-CPh$)(\mu_3$-COMe)[5]. The ^{1}H NMR spectrum of 2 shows the phenyl protons in the range δ 7.86–7.24 (10 H) with the same type of pattern as that observed for 1, whereas a 6 H single at δ 3.76 is assigned to the methoxy protons.

The ^{13}C NMR spectrum of $Os_3(*CO)_8(\eta^1$-*C(OMe)$_2)(\mu_3$-*CPh$)_2$ is shown in Figure 2. Resonances at δ 268.4 and 220.4 in a ratio approximately 2:1 are assigned to the benzylidyne and dimethoxycarbene carbons, respectively. The two-carbon signal at δ 180.8 is assigned to the two carbonyls in the $Os(CO)_2$(=C(OMe)$_2$) group, and the six-carbon singlet at δ 178.0 to the remaining six

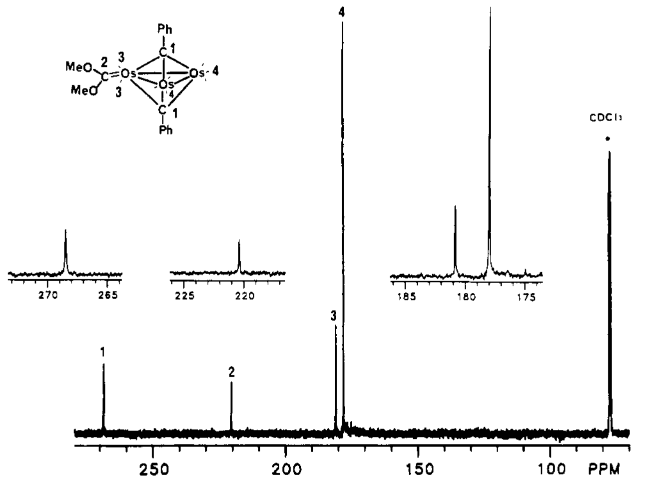

Figure 2. 90 MHz ^{13}C NMR spectrum of $Os_3(*CO)_8(\eta^1\text{-}*C(OMe)_2)(\mu_3\text{-}*CPh)_2$ in $CDCl_3$ at −55 °C.

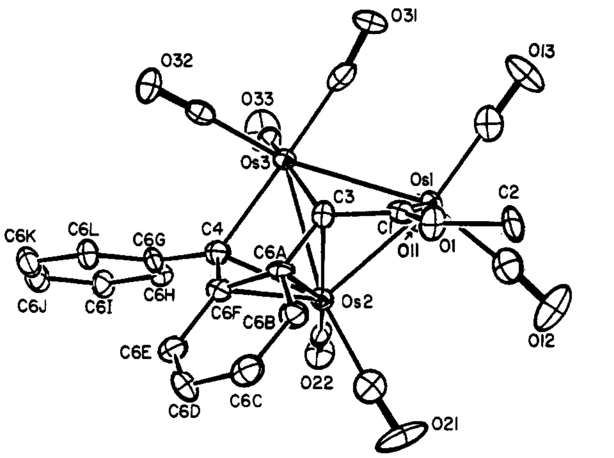

Figure 3. Labeling of atoms in the $Os_3(CO)_8(\mu_3,\eta^5\text{-}C(OMe)C(1,2\text{-}C_6H_4CPh))$ molecule (ORTEP-II diagram, with hydrogen atoms artificially reduced).

carbonyls in the two equivalent $Os(CO)_3$ groups. The shift difference is 2.8 ppm. This slightly downfield shift for the carbonyl carbons adjacent to the substitutent was also noted for $Os_3(CO)_8(\eta^1\text{-}C(OMe)Ph)(\mu_3\text{-}CPh)(\mu_3\text{-}COMe)$ ($\Delta\delta$ = 3.8 ppm)[16] and $Os_3(CO)_8(PPh_3)(\mu_3\text{-}CPh)(\mu_3\text{-}COMe)$ ($\Delta\delta$ = 7.8 ppm).[5] It would appear that the increase of downfield shits from $\Delta\delta$ = 2.8 to 7.8 ppm reflects the increasing ligand basicity in the order CO < $C(OMe)_2$ < C(OMe)Ph < PPh_3.

Description of the Crystal Structure of $Os_3(CO)_8(\mu_3,\eta^5\text{-}C(OMe)C(1,2\text{-}C_6H_4CPh))$ (3). The crystal consists of discrete molecular units of $Os_3(CO)_8(\mu_3,\eta^5\text{-}C(OMe)C(1,2\text{-}C_6H_4CPh))$ separated by normal van der Waals' distances; there are no abnormally short intermolecular contacts. The individual molecules are inherently chiral, but the crystal contains equal numbers of the two enantiomers by virtue of the inversion centers and *c*-glide operations of space group $P2_1/c$. Figure 3 shows the molecule projected onto the triosmium plane and gives the system used in labeling the non-hydrogenic atoms. Interatomic distances and their esd's are collected in Table III. The table of bond angles, with esd's, is deposited as supplementary material. A stereoscopic view of the molecule is provided in Figure 4.

The three osmium atoms define a triangular cluster in which the individual bond lengths, in increasing order, are Os(2)–Os(3) = 2.720 (1) Å, Os(1)–Os(2) = 2.754 (1) Å, and

Table III. Interatomic Distances (Å) with Esd's for $Os_3(CO)_8(\mu_3,\eta^5\text{-}C(OMe)C(1,2\text{-}C_6H_4CPh))$

(A) Os–Os Bond Lengths			
Os(1)–Os(2)	2.754 (1)	Os(1)–Os(3)	2.903 (1)
Os(2)–Os(3)	2.720 (1)		
(B) Os–CO and Associated C–O Bond Lengths			
Os(1)–C(11)	1.936 (19)	C(11)–O(11)	1.136 (24)
Os(1)–C(12)	1.857 (19)	C(12)–O(12)	1.154 (24)
Os(1)–C(13)	1.866 (18)	C(13)–O(13)	1.168 (22)
Os(2)–C(21)	1.911 (17)	C(21)–O(21)	1.133 (21)
Os(2)–C(22)	1.853 (15)	C(22)–O(22)	1.164 (19)
Os(3)–C(31)	1.918 (17)	C(31)–O(31)	1.184 (20)
Os(3)–C(32)	1.928 (15)	C(32)–O(32)	1.129 (19)
Os(3)–C(33)	1.945 (16)	C(33)–O(33)	1.128 (21)
(C) Os-(μ_3,η^5-C(OMe)C(1,2-C_6H_4CPh) Bond Lengths			
Os(1)–C(1)	2.065 (13)	Os(2)–C(6F)	2.326 (13)
Os(2)–C(3)	2.240 (12)	Os(3)–C(3)	2.117 (13)
Os(2)–C(4)	2.162 (14)	Os(3)–C(4)	2.161 (14)
Os(2)–C(6A)	2.331 (12)		
(D) Distances within Carbocyclic Rings			
C(6A)–C(6B)	1.456 (20)	C(6G)–C(6H)	1.386 (20)
C(6B)–C(6C)	1.352 (21)	C(6H–C(6I)	1.375 (20)
C(6C)–C(6D)	1.426 (23)	C(6I)–C(6J)	1.389 (23)
C(6D)–C(6E)	1.346 (22)	C(6J)–C(6K)	1.373 (24)
C(6E)–C(6F)	1.439 (20)	C(6K)–C(6L)	1.389 (22)
C(6F)–C(6A)	1.444 (20)	C(6L)–C(6G)	1.362 (20)
(E) Other Intraligand Distances			
C(1)–O(1)	1.303 (18)	C(6A)–C(6F)	1.444 (20)
C(2)–O(1)	1.468 (18)	C(6F)–C(4)	1.412 (20)
C(1)–C(3)	1.449 (20)	C(4)–C(6G)	1.532 (20)
C(3)–C(6A)	1.399 (18)		

Os(1)–Os(3) = 2.903 (1) Å (cf. Os–Os(av) = 2.877 (3) Å in the parent binary carbonyl, $Os_3(CO)_{12}$).[17] The individual osmium atoms are each associated formally with 18 outer valence electrons, and the cluster as a whole is associated with the 48 electrons expected for a triangular metal cluster complex. The variation in Os–Os bond length appears to correlate only slight with the length of bridges from the μ_3,η^5-C(OMe)C(1,2-C_6H_4CPh) ligand spanning the Os–Os bonds. Thus, the shortest such bond length (for Os(2)–Os(3)) is associated with the one-atom bridges Os(2)–Os(3)–Os(3) and Os(2)–C(4)–Os(3). However, the remaining two Os–Os bonds are each bridged by two atoms (-C(1)–C(3)-), but have bond lengths varying by approximately 0.15 Å (i.e., Os(1)–Os(2) = 2.754 (1) Å vs. Os(1)–Os(3) = 2.903 (1) Å). The difference in these bond lengths must result from differences in the ligand environment at Os(2) and Os(3).

Os(1) and Os(3) are each associated with three terminal carbonyl ligands, while Os(2) has only two. Osmium–carbonyl distances range from 1.853 (15) through 1.945 (16) Å, averaging 1.902 ± 0.037 Å. No two carbonyl ligands are in equivalent environments, so, unlike the case of $Os_3(CO)_{12}$ (wherein Os–CO (axial) distances average 1.946 ± 0.006 Å and are systematically longer than the Os–CO (equatorial) distances, which average 1.912 ± 0.007 Å), they do not break down into obvious subsets. The C–O distances range from 1.128 (21) Å through 1.184(20) Å, averaging 1.150 ± 0.021 Å.

We now turn our attention to the μ_3,η^5-C(OMe)C(1,2-C_6H_4CPh) ligand. This ligand is bound to Os(1) via a terminal alkylidene linkage, with Os(1)=C(1) = 2.065 (13) Å (cf. Os=$C(OMe)_2$ = 2.039 (18) Å in the species (μ-H)-$Os_3(CO)_9(\eta^1\text{-}C\text{-}(OMe)_2)(\mu\text{-}CPh)$[3]); there is clearly some multiple-bond character in the C(1)–O(1) linkage as evidenced by its contraction relative to the O–Me linkage (i.e., C(1)–O(1) = 1.303 (18) Å, compared to O(1)–C(2) = 1.468

(16) Yeh, W.-Y.; Shapley, J. R., unpublished results.

(17) Churchill, M. R.; DeBoer, B. G. *Inorg. Chem.* **1977**, *16*, 878.

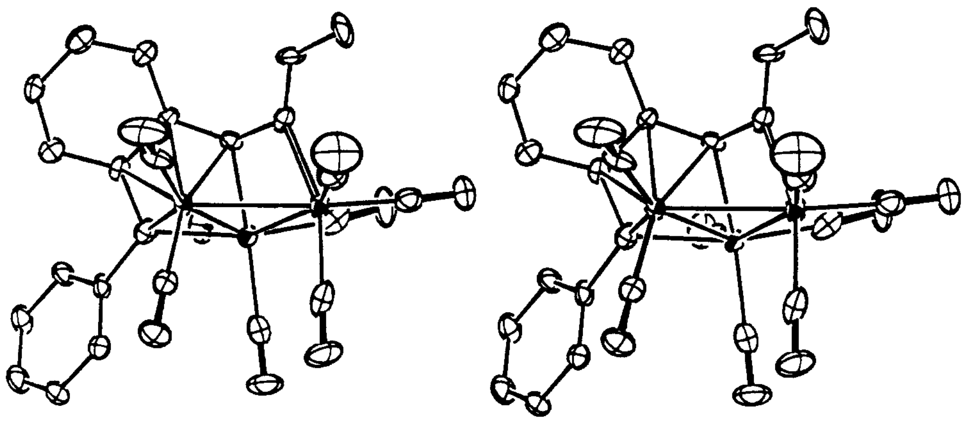

Figure 4. A stereoscopic view of the $Os_3(CO)_8(\mu_3,\eta^5\text{-}C(OMe)C(1,2\text{-}C_6H_4CPh)$ molecule.

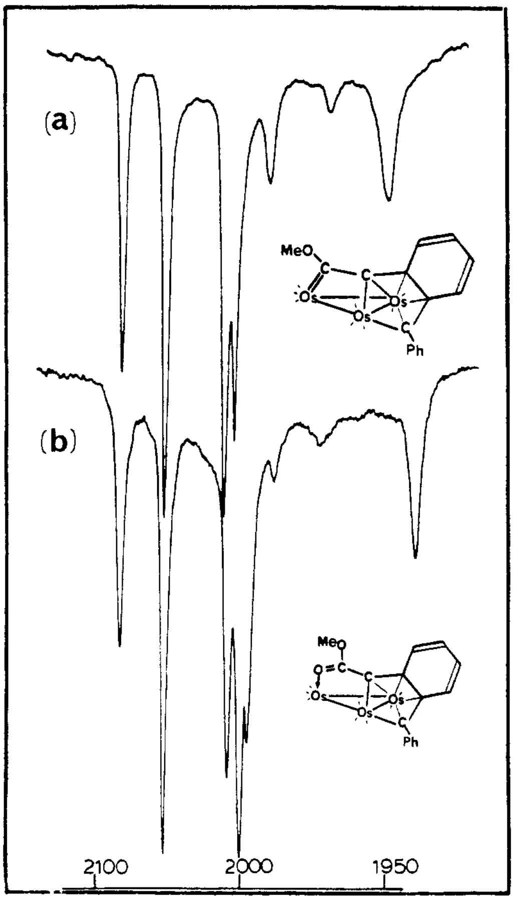

Figure 5. IR spectra in the carbonyl region of (a) $Os_3(CO)_8(\mu_3,\eta^5\text{-}C(OMe)C(1,2\text{-}C_6H_4CPh))$ and (b) $Os_3(CO)_8(\mu_3,\eta^5\text{-}C(O)(OMe)C(1,2\text{-}C_6H_4CPh))$; obtained in C_6H_{12}.

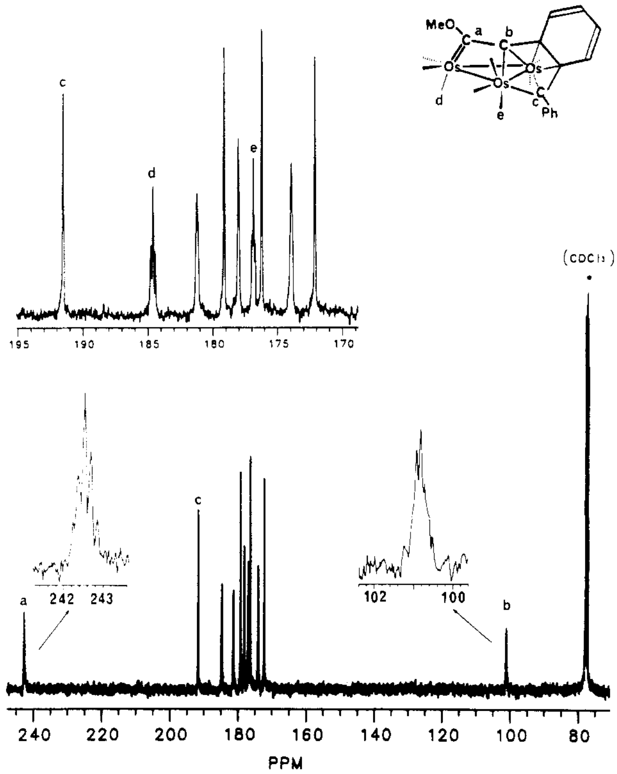

Figure 6. 90 MHz ^{13}C NMR spectrum of $Os_3(^*CO)_8(\mu_3,\eta^5\text{-}^*C(OMe)^*C(1,2\text{-}C_6H_4{}^*CPh))$ in $CDCl_3$ at −55 °C.

(18) Å). Angles at C(1) are Os(1)–C(1)–C(3) = 104.3 (9)°, Os(1)–C(1)–O(1) = 138.3 (10)°, and C(3)–C(1)–O(1) = 116.8 (12)° ($\sum$ = 359.4°, indicative of planarity about C(1)). Atom C(3) bridges Os(2) and Os(3) with Os(2)–C(3) = 2.240 (12) Å and Os(3)–C(3) = 2.117 (13) Å and is linked both to the =C(OMe) group (C(3)–C(1) = 1.449 (20) Å) and to the 1,2-C_6H_4 fragment (C(3)–C(6A) = 1.399 (18) Å). This atom has a very distorted tetrahedral geometry, with interatomic angles of Os(2)–C(3)–C(6A) = 75.8 (8)°, Os(2)–C(3)–Os(3) = 77.2 (4)°, Os(2)–C(3)–C(1) = 94.1 (8)°, Os(3)–C(3)–C(1) = 111.2 (9)°, Os(3)–C(3)–C(6A) = 118.3 (9)°, and C(1)–C(3)–C(6A) = 125.1 (12)°. For this reason it is best to regard both C(3) and C(4) (which, formally, bridges Os(2) and Os(3), with Os(2)–C(4) = 2.162(14) Å and Os(3)–C(4) = 2.161(14) Å), along with atoms C(6A) and C(6F) of the 1,2-C_6H_4 moiety and Os(3) as forming a planar osmacyclopentadiene ligand which coordinates to the $Os(CO)_2$ system centered on Os(2).

The utilization of atoms C(6A) and C(6F) in binding to Os(2) destroys the aromaticity of the 1,2-C_6H_4 system. There is localization of π-electron density as indicated by alternating long and short C–C bonds around the noncoordinated atoms (C(6A)–C(6B) = 1.456 (20) Å, C(6B)–C6C) = 1.352 (21) Å, C(6C)–C(6D) = 1.426 (23) Å, C(6D)–C(6E) = 1.346 (22) Å, and C(6E)–C(6F) = 1.439 (20) Å). No such alternation occurs in the other six-membered ring, defined by C(6G)→C(6L), where C–C distances range only from 1.362 (20) Å through 1.389 (22) Å, averaging 1.379 ± 0.011 Å.

Spectroscopic Characterization of Compound 3. The IR spectrum in the carbonyl region of 3 is illustrated in Figure 5a. This absorption pattern is similar to that observed for $(\mu\text{-}H)Os_3(CO)_8(\mu_3,\eta^5\text{-}C(R)(CPh)_2C(1,2\text{-}C_6H_4))$ (R = OMe,[16] Ph[18]), where an osmacyclopentadiene moiety

(18) Gambino, O.; Vaglio, G. A.; Ferrari, R. P.; Getini, G. *J. Organomet. Chem.* 1971, *30*, 381.

is indicated. The ^1H NMR spectrum of **3** shows the phenyl protons as a complex multiplet in the range δ 7.84–7.34 (9 H) and the methoxy protons at δ 4.25 (3 H).

The ^{13}C NMR spectrum of $Os_3(*CO)_8(\mu_3,\eta^5$-*C(OMe)-*C(1,2-C_6H_4*CPh)) (each enriched site ca. 50% ^{13}C) is shown in Figure 6. There are eight carbonyl resonances in the range δ 184.6–172.1. The carbene carbon (a) is assigned to the signal at δ 242.5,[19] which shows coupling to the axial carbonyl carbon (d) at δ 184.6 (^2J(C–C) = 30 Hz), and to the adjacent carbon (b) at δ 100.8 (^2J(C–C) = 31 Hz). The carbon (b) is also coupled to a carbonyl carbon (e) at δ 176.8 (^2J(C–C) = 20 Hz). The signal at δ 191.5 is assigned to the carbon (c).

Characterization of Compound 4. The IR (Figure 5b) and ^1H NMR spectra of $Os_3(CO)_8(\mu_3,\eta^5$-C(O)(OMe)C(1,2-C_6H_4CPh)) (**4**) are in close agreement with those observed for $Os_3(CO)_8(\mu_3,\eta^5$-C(OMe)C(1,2-C_6H_4CPh)) (**3**), suggesting a related configuration for both compounds. Therefore, based on the structure determined for **3**, a structure for **4** can be proposed as shown in Figure 5b, in which a C(O)OMe group replaces a COMe group. This μ-acetyl bonding mode is quite common in cluster complexes.[19,20]

(19) (a) Jensen, C. M.; Knobler, C. B.; Kaesz, H. D. *J. Am. Chem. Soc.* **1984**, *106*, 5926. (b) Jensen, C. M.; Lynch, T. J.; Knobler, C. B.; Kaesz, H. D. *J. Am. Chem. Soc.* **1982**, *104*, 4679.

Conclusions

It appears that sequential Ph^-/Me^+ treatment is effective for transformation of carbonyl ligands to alkylidene and alkylidyne moieties. Furthermore, by repeating this two-step procedure, dialkylidyne and mixed alkylidene–alkylidyne complexes can be prepared. The overall predictability of the treatment, however, is low.

Acknowledgment. This research was supported at the University of Illinois by NSF Grant CHE 84-07233 to J.R.S. Mass spectra were obtained at the University of Illinois in part under a grant from the National Institute of General Medical Science (GM 27029).

Registry No. 1, 105103-50-2; 2, 105103-51-3; 3, 105103-52-4; 4, 105121-17-3; (μ-H)$Os_3(CO)_9(\eta^1$-C(OMe)$_2$)(μ_3-CPh), 105181-34-8; (μ-H)$Os_3(CO)_{10}(\mu_3$-CPh), 95122-80-8; Os, 7440-04-2.

Supplementary Material Available: Tables of internuclear bond angles and anisotropic thermal parameters for compound 3 (4 pages); a listing of observed and calculated structure factors (16 pages). Ordering information is given on any current masthead page.

(20) (a) Azam, K. A.; Deeming, A. J.; Rothwell, I. P *J. Chem. Soc., Dalton Trans.* **1981**, 91. (b) Keister, J. B.; Shapley, J. R. *J. Am. Chem. Soc.* **1976**, *98*, 1056. (c) Strickland, D. S. Ph.D. Thesis, University of Illinois, 1983.

Crystal Structures of Organotungsten Complexes Formed by Sequential Insertion of Elemental Sulfur into Tungsten–Carbon Bonds

Stephen V. Evans, Peter Legzdins,* Steven J. Rettig, Luis Sanchez, and James Trotter*

Department of Chemistry, University of British Columbia, Vancouver, British Columbia, Canada V6T 1Y6

Received May 8, 1986

The novel organotungsten complexes $(\eta^5-C_5H_5)W(NO)(SR)R$ (**1**) and $(\eta^5-C_5H_5)W(NO)(\eta^2-S_2R)R$ (**2**) (R = CH_2SiMe_3) result from the sequential insertion of elemental sulfur into W–C σ bonds of $(\eta^5-C_5H_5)W(NO)R_2$. The molecular structures of **1** and **2** have been established by crystal structure analyses. Crystals of **1** are monoclinic, $P2_1/c$, with a = 12.992 (3) Å, b = 12.726 (1) Å, c = 11.937 (2) Å, β = 98.810 (8)°, and Z = 4; the structure was solved by conventionial heavy-atom methods and was refined by full-matrix least-squares procedures to R = 0.036 and R_w = 0.044 for 3195 absorption-corrected reflections with $I \geq 3\sigma(I)$. Crystals of **2** are also monoclinic, $P2_1/c$, with a = 13.223 (1) Å, b = 12.685 (1) Å, c = 12.113 (1) Å, β = 92.942 (5)°, and Z = 4; R = 0.038 and R_w = 0.040 for 2546 reflections. Both complexes are monomeric and possess "piano stool" molecular structures; in **1**, a short (2.301 (2) Å) W–S bond indicates significant multiple-bond character in this formally 16-electron complex, while **2** is an 18-electron complex, with the η^2-S_2R ligand functioning as a formal three-electron donor, W–S = 2.479 (2) and 2.453 (3) Å.

Introduction

Metal complexes containing chalcogenides in their framework are of synthetic and theoretical interest due to their apparent involvement in various biological and catalytic processes.[1] The experimental conditions for effecting the transformations (where M = $(\eta^5-C_5H_5)W(NO)$ and R = CH_2SiMe_3) and the characterization of the novel complexes **1**–**3** by conventional spectroscopic methods have been described.[2] The spectroscopic data, however, not

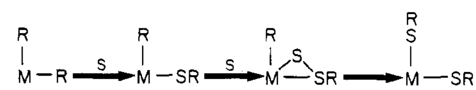

1 2 3

only were consistent with the formulations of **1** and **2** shown in eq 1, but also were in accord with **1** being a dimer

(1) Gautheron, B.; Tainturier, G.; Pouly, S.; Theobald, F.; Vivier, H.; Laarif, A. *Organometallics* **1984**, *3*, 1495.

(2) Legzdins, P.; Sanchez, L. *J. Am. Chem. Soc.* **1985**, *107*, 5525.

